KSME Journal, Vol. 10, No. 2, pp. 169~179, 1996

$H\infty$ Control for Flutter Suppression of a Laminated Plate with Self-Sensing Actuators

Jong-Sun Kim* and Changho Nam**

(Received June 12, 1995)

Active flutter suppression system of a composite plate wing model is designed using a reduced order model. The analysis for a laminated composite wing with segmented piezoelectric sensor/actuator pairs is conducted by the Ritz solution technique. Unsteady aerodynamic forces calculated by doublet lattice method are approximated as the transfer functions of the Laplace variable by the minimum state method. Among the aerodynamic states obtained from rational function approximation, only one aerodynamic state is included in the plant model for feedback purpose. The neglected aerodynamic states are regarded as modeling error. The control system uses the integrated and collocated piezoelectric self-sensing actuator pairs so as to prohibit the non-minimum phase model and the spillover due to the unmodeled dynamics. Based on the mixed-sensitivity H_∞ control method, the control parameters are determined. Using a simple wing model, the performance of the controlled system is shown in the frequency and time domain respectively. The electric current and the power requirement for aeroelastic control are also predicted.

Key Words : Aeroelasticity, Flutter Suppression, Reduced Order Model, H∞ Control, Self-Sensing Actuator.

1. Introduction

There has been a considerable amount of research activity to use piezoelectric materials as sensor/actuators for the response control of structures. The piezoelectric materials generate an electrical charge (direct effect) in proportion to the applied mechanical forces and vice versa (converse effect). Due to the direct and converse effects of piezoelectric materials, the intelligent structure which is defined as a structure with the integrated sensor/actuator system is possible. The application of the intelligent structure by the use of sensor/actuator shows the potential to enhance the structural performance as well as reliability. Recently, Zhou et. al. (1994) developed a theoretical model to predict and analyze the power requirement and power consumption of the system. They also conducted the experiment and verified their analytical results.

A number of investigators (Ehlers et. al., 1992; Lin et. al. 1994, Leeks et. al., 1994, Suleman et. al., 1994) have studied the static and dynamic aeroelastic control of wing structure with piezo actuators and demonstrated the feasibility of the application of piezoelectric materials. The application of piezoelectric materials to aeroelastic control may provide a new dimension in design to eliminate the instability by changing wing configuration to cause lift distribution variation. The optimization technique was applied to find the best geometry of the piezo actuators for the aer-

*Department of Mechanical Engineering & Design, Hankuk Aviation University, 200-1, Hwajon-Dong, Teokyang-Ku, Koyang-shi, 411-791, Korea

**Department of Aeronautical & Mechanical Engineering, Hankuk Aviation University, 200-1, Hwajon-Dong, Teokyang-Ku, Koyang-shi, 411-791, Korea

oelastic control (Leeks et. al., 1994, Nam et. al., 1995).

The usual approach in the design of the active flutter suppression system was to use articulated control surfaces as actuators. The choice of articulated control surfaces is primarily due to the availability of actuators on the majority of current aircraft and not their desirability as actuators. In this research, the strain actuators are used to apply control forces directly to the lifting surface. Based on the results of our previous study (Nam and Kim, 1995, Nam et. al., 1995), a robust controller is designed for active flutter suppression using the reduced order model. The analysis for a laminated composite wing with segmented piezoelectric sensor/actuator pairs is conducted by Ritz solution technique. The active control system design for flutter suppression requires equations of motion to be expressed in a linear time-invariant state-space form. Doublet lattice method is used to compute unsteady aerodynamic forces, which are approximated as the transfer functions of the Laplace variable by minimum state method combined with optimization technique. In order to design an active control system efficiently, the plant should be modeled accurately. However, this requires to increase the number of state variables for the rational function approximation of the unsteady aerodynamic forces. There is always a trade-off between the cost for real-time implementation and performance of the controlled system. Among the aerodynamic states obtained from rational function approximation, only one aerodynamic state is included in the plant model for feedback purpose. The neglected aerodynamic states are regarded as a modeling error. The control system uses the integrated and collocated piezoelectric self-sensing actuator pairs so as to prohibit the non-minimum phase model as well as the spillover due to the unmodeled dynamics. Based on the mixed-sensitivity H_∞ control method, the control parameters are determined. This method enables one to achieve not only the disturbance attenuation specification but also the stability margin specification with the unstructured modeling error, which are combined into a single infinity norm specification (Glover et. al., 1989, Doyle et. al., 1989). Using a simple wing model, the performance of the controlled system is shown in the frequency and time domain, respectively. The electric current and the input control voltage which are required for aeroelastic control are also examined.

2. Modeling of the Wing Structure

Based on the classical laminated plate theory, the equations of motion of a model with piezo actuators are formulated. For the design of the flutter suppression system, a composite wing model which has four pairs of the self-sensing piezoelectric actuators on the surface is considered as shown in Fig. 1. The model is assumed to be a symmetric laminated plate and has the same size of the surface bonded piezoelectric materials on the top and bottom of plate at the same location.

The linear coupled electromechanical constitutive relations of a piezoelectric materials can be written as ;

$$\{D\}=[d]^T\{T\}+[\varepsilon^T]\{E\} \tag{1a}$$

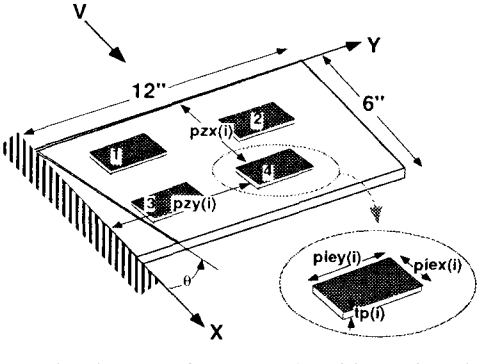

Fig. 1 Laminated plate model with self-sensing actuators.

$$\{S\}=[s^E]\{T\}+[d]\{E\} \tag{1b}$$

$\{S\}$ is the strain, $\{T\}$ is the stress, $\{D\}$ is the electric displacement, and $\{E\}$ is the electric field intensity. $[d]$, $[\epsilon^T]$, $[s^E]$ denote the piezoelectric strain constant, dielectric constant, and elastic compliance matrix, respectively. It is assumed that the "3" axis is associated with the direction of poling and the mechanical property of the piezoelectric materials is modeled as an isotropic material. For the thin plate shape of the piezoelectric materials, we can rewrite Eq. (1).

$$D_3=\lceil d_{31}\ d_{32}\ 0\rfloor\lceil\sigma_{xx}\ \sigma_{yy}\ \sigma_{xy}\rfloor^T + \varepsilon_{33}^T E_3 \tag{2a}$$

$$\begin{Bmatrix}\epsilon_{xx}\\ \epsilon_{yy}\\ \gamma_{xy}\end{Bmatrix}=\begin{bmatrix}s_{11} & s_{12} & 0\\ s_{12} & s_{22} & 0\\ 0 & 0 & s_{66}\end{bmatrix}\begin{Bmatrix}\sigma_{xx}\\ \sigma_{yy}\\ \sigma_{xy}\end{Bmatrix} + \begin{Bmatrix}d_{31}\\ d_{32}\\ 0\end{Bmatrix}E_3 \tag{2b}$$

where $d_{31}=d_{32}$. The electric charge which is the output signal can be obtained by integrating the electric displacement D_3 with respect to the area of piezo actuators. The electric current is calculated by taking derivative of the charge with respect to time.

Strain energy and kinetic energy of the composite wing model with piezoelectric actuators can be expressed as;

$$U=\frac{1}{2}\iint_{A,\ A_P}\lfloor\ \epsilon\ \kappa\rfloor\begin{bmatrix}A_S & B_S\\ B_S & D_S\end{bmatrix}\begin{Bmatrix}\epsilon\\ \chi\end{Bmatrix}dx\ dy - \iint_{A_P}\lfloor\ N_A\ M_A\rfloor\begin{Bmatrix}\epsilon\\ \chi\end{Bmatrix}dx\ dy \tag{3}$$

$$T=\frac{1}{2}\iint_{A,\ A_P}\rho(\dot{u}^2+\dot{v}^2+\dot{w}^2)\,dx\ dy \tag{4}$$

where A, A_P represent area of composite plate and piezoelectric actuator, respectively. $\{\epsilon\}$, $\{\kappa\}$ are the midplane strain and curvature. $[A_S]$, $[D_S]$, and $[B_S]$ are extension, bending, and extension/bending coupling stiffness matrices, respectively. $\{N_A\}$ and $\{M_A\}$ are inplane forces and moments due to actuator strain, ρ is the mass per unit area, u, v, w are displacements in x, y, z direction. The virtual work due to aerodynamic forces is

$$\delta W_A=\iint_A \Delta p\ \delta w dx dy \tag{5}$$

where Δp is the pressure and δw is the virtual displacement. The aerodynamic force is calculated using the doublet-lattice method (Albano et. al., 1969) for Mach 0.8 and 15 reduced frequencies ranging from 0 to 1.5.

The Ritz solution technique is used for the structural analysis. The Ritz solution technique assumes a deflection shape for the wing structure. In this paper, it is assumed that the same magnitude but the opposite direction of electric field is applied to the piezoelectric material so as to create a pure bending moment for flutter control. With this assumption, the inplane displacements can be neglected. The out-of-plane displacement w on the model is represented as a set of polynomial functions and written as;

$$w(x,\ y,\ t)=\sum_{k=1}^{n} Z_k(x,\ y)\,q_k(t) = \lfloor Z\rfloor\{q\} \tag{6}$$

where $\{q\}$ is the generalized coordinate. The displacement functions Z_k are assumed as products of polynomial in x and y directions. The assumed displacement functions are chosen to satisfy the geometric boundary conditions for a wing clamped at the root.

$$Z_k(x,\ y)=\left(\frac{x}{X_{max}}\right)^i\left(\frac{y}{Y_{max}}\right)^j,\quad i=0,\ 1,\ 2,\ 3,\ \cdots,\ j=2,\ 3,\ 4,\ 5,\ \cdots \tag{7}$$

where X_{max} and Y_{max} are constant normalization length. These are defined as the root chord and span, respectively. Using these displacement expressions, the strain energy and kinetic energy are written in a matrix form;

$$U=\frac{1}{2}\{q\}^T[K_S]\{q\}-\lfloor Q_A\rfloor\{q\} \tag{8}$$

$$T=\frac{1}{2}\{\dot{q}\}^T[M_S]\{\dot{q}\} \tag{9}$$

where $[K_s]$ and $[M_s]$ are the stiffness, mass matrices respectively. $\{Q_A\}$ is $[F_p]\{u\}$. $[F_p]$ is the control force matrix due to unit electric voltage, and $\{u\}$ is the applied voltage. The virtual work in the generalized coordinate is $\delta W_A = Q_{Ai}\delta q_i$. The generalized aerodynamic force $\{Q_A\}$ is expressed as $q_d[A]\{q\}$. q_d is the dynamic pressure and $[A]$ is the unsteady aerodynamic force matrix.

Lagrange's equation results in a set of ordinary differnetial equations of motion. After the vibration analysis, a model reduction is performed using first 6 vibration modes to obtain a set of equations of motion in modal coordinates. Then, the reduced equations of motion is as following form ;

$$[\bar{M}_s]\{\ddot{\bar{q}}\}+[\bar{K}_s]\{\bar{q}\} = [\bar{F}_p]\{u\}+q_d[\bar{A}]\{\bar{q}\} \tag{10}$$

where $[\bar{M}_s]=[\Phi]^T[M_s][\Phi]$, $[\bar{K}_s]=[\Phi]^T[K_s][\Phi]$, $[\bar{A}_s]=[\Phi]^T[A_s][\Phi]$, and $[\bar{F}_p]=[\Phi]^T[F_p]$. $[\Phi]$ is a matrix of the individual eigenvectors ϕ_i. $\{\bar{q}\}$ represents the modal coordinate.

The signal obtained from the self-sensing actuators with charge amplifier is used as the output vector. The output vector is written as ;

$$\{y_Q\} = k_s\int_{A_{pi}} D_3 dxdy = k_s[\bar{F}_p]^T\{\dot{\bar{q}}\}+k_s[D]\{\dot{u}\} \tag{11}$$

where k_s is the gain of the charge amplifier. From Eq. (2), the observation matrix is proportional to the transpose of the control matrix. $[D]$ is the diagonal matrix and the components of $[D]$ are given as ;

$$D_{ii} = -\frac{2A_{pi}}{t_{pi}}\left(\varepsilon_{33}^T - \frac{2d_{31}^2 E_p}{1-\nu_p}\right),\ d_{31}=d_{32} \tag{12}$$

where ν_p and E_p are the poisson's ratio and Young's modulus of the piezoelectric materials, A_{pi}, t_{pi} is the area, thickness of the i-th piezoelectric actuator. The electric currents flowing through the piezoelectric actuators can be obtained by taking time derivative of the electric charge stored due to the direct effect of the piezoelectric materials. Since $I_i = \int_{A_{pi}} \dot{D}_3 dxdy$, the current vector is written as ;

$$\{I\} = [\bar{F}_p]^T\{\ddot{\bar{q}}\}+[D]\{\dot{u}\} \tag{13}$$

For aeroservoelastic analysis and design, it is necessary to transform the equations of motion into the state space form. This requires approximating the unsteady aerodynasmic forces in terms of rational functions of the Laplace variable. There are several methods for the rational function approximation (RFA), but RFA always causes an increase in the total number of states due to the addition of augmented aerodynamic states to represent unsteady aerodynamic forces accurately. In this study, minimum state method (Hoadley et. al., 1991) combined with optimization technique is adopted for the rational function approximation, since the increase in the size of the augmented aerodynamic state is smaller than any other methods.

Minimum state method (Hoadley et. al., 1991) approximates the aerodynamic force matrix by

$$[\bar{A}_{ap}(\bar{s})] = [\bar{A}_0]+[\bar{A}_1]\bar{s}+[\bar{A}_2]\bar{s}^2 + [D'_a][\bar{s}I - R'_a]^{-1}[E_a]\bar{s} \tag{14}$$

where the nondimensionalized Laplace variable $\bar{s}=(sb/V)$, V is the air speed, b is the semi chord, and s is the Laplace variable. The components of the diagonalized matrix $[R'_a]$ are negative constants which are selected arbitrarily. For given $[R'_a]$ matrix, $[\bar{A}_0]$, $[\bar{A}_1]$, $[\bar{A}_2]$, $[D'_a]$, and $[E_a]$ are determined by using repeated least-square fit.

Using Eq. (14) for the RFA and the state vector $\{x_f\}^T = \lfloor \bar{q}\ \ \dot{\bar{q}}\ \ q_a \rfloor$, the state equation (full model) which includes the effects of piezoelectric control forces is expressed as follows ;

$$\{\dot{x}_f\} = [\tilde{A}_f]\{x_f\}+[\tilde{B}_f]\{u\} \tag{15}$$

$$\{y_f\} = [\tilde{C}_f]\{x_f\}+[\tilde{D}_f]\{u\} \tag{16}$$

where

$$[\tilde{A}_f] = \begin{bmatrix} [0] & [I] & [0] \\ -[\bar{M}]^{-1}[\bar{K}] & -[\bar{M}]^{-1}[\bar{B}] & -[\bar{M}]^{-1}[D_a] \\ [0] & [E_a] & [R_a] \end{bmatrix} \tag{17a}$$

$$[\tilde{B}_f]=\begin{bmatrix}[0]\\ [\bar{M}]^{-1}[\bar{F}_p]\\ [0]\end{bmatrix} \tag{17b}$$

$$[\tilde{C}_f]=\begin{bmatrix}k_s[\bar{F}_p]^T\ [0]\ [0]\end{bmatrix} \tag{17c}$$

$$[\tilde{D}_f]=[0] \tag{17d}$$

It could be noted that the auxiliary output $\{y_f\}$ is specified so as to make the system be strictly proper. The detailed expressions for $[\bar{M}]$, $[\bar{B}]$, $[\bar{K}]$, $[D_a]$, and $[R_a]$ can be found in the literature (Num et. al., 1995). q_a is the aerodynamic state vector. If $[R'_a]$ is set to be a $m\times m$ matrix, the total number of states is $12+m$. A total of 6 components of $[R'_a]$ matrix are used for the RFA. Therefore, the dimension of the state vector is 18.

3. The Robust Controller Design

3.1 Reduced order model

Since the system matrix is a function of the dynamic pressure, it is necessary to choose the design air speed for designing control system. Approximating high order plant and controller models to lower order models is an integral part of control system design. Complicated plant models lead to high order controllers and the difficulties associated with implementing them. The reduced order models simplify the process of understanding the design limitations. Also, the controller synthesis computations become faster and require less memory. In this study, model reduction is performed to truncate unimportant states from the full state model. The aerodynamic stiffness, damping, mass matrices, ($[\bar{A}_0]$, $[\bar{A}_1]$, $[\bar{A}_2]$) have influence on the stability of the system over entire frequency range. These matrices are included in the reduced order model. We considered one of the aerodynamic states, which is a dominant state, as the equivalent aerodynamic state and other aerodynamic states are considered as modeling error. In this paper, the model reduction is performed with the stable modes by using the internal balancing method (Moore, 1981). The reduced order model (control model) is written as follows;

$$\{\dot{x}\}=[\tilde{A}]\{x\}+[\tilde{B}]\{u\} \tag{18}$$

$$\{y\}=[\tilde{C}]\{x\}+[\tilde{D}]\{u\} \tag{19}$$

where $[\tilde{A}]$ is the system matrix of the reduced model which includes the twelve structural states and one aerodynamic state. The input/output relation can be obtained by taking the Laplace transform of the full (Eqs. 15, 16) and control (Eqs. 18, 19) models. The results are written in frequency domain;

$$\begin{aligned}\{y(s)\}&=[\hat{G}_f(s)]\{u(s)\}\\ &=[I+\Delta(s)]\left[\hat{G}(s)\right]\{u(s)\}\end{aligned} \tag{20}$$

where

$$[\hat{G}_f(s)]=[\tilde{C}_f][sI-\tilde{A}_f]^{-1}[\tilde{B}_f]+[\tilde{D}_f] \tag{21a}$$

$$[\hat{G}(s)]=[\tilde{C}][sI-\tilde{A}]^{-1}[\tilde{B}]+[\tilde{D}] \tag{21b}$$

$$[\Delta(s)]=[\hat{G}_f(s)][\hat{G}(s)]^{-1}-[I] \tag{21c}$$

$[\Delta(s)]$ is the unstructured multiplicative modeling error, which might include the neglected aerodynamic states from the model reduction.

The robust stability about the modeling error is given as follows;

$$\bar{\sigma}([\Delta(jw)])<\frac{1}{\bar{\sigma}([T(jw)])},\quad \forall\ w>0 \tag{22}$$

where $\bar{\sigma}(.)$ denotes maximum singular value and $[T]$ is the closed loop transfer function matrix.

3.2 H_∞ controller design

Figure 2 shows the closed loop system considering a multiplicative modeling error (Safonov et. al., 1989). In Fig. 2, the transfer matrix $[\hat{G}]$, and $[K]$, $[W_1]$, $[W_3]$, $[\Delta]$ are square matrices. The H_∞ norm defined in frequency domain for a transfer matrix is written as follows;

$$\|[\hat{G}]\|_\infty=\sup_w \bar{\sigma}([\hat{G}(jw)]) \tag{23}$$

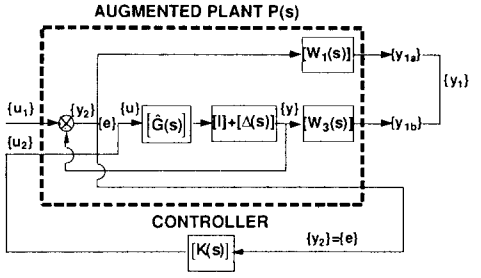

Fig. 2 Block diagram of robust control system.

A standard H_∞ problem is to find the controller $[K]$ such that the H_∞ norm of the closed loop transfer function matrix $[T_{y1u1}]$ is to satisfy the inequality (Safonov et. al., 1989) ;

$$Find \underset{[K]stabilizing}{Inf} \| [T_{y1u1}] \|_\infty < 1 \tag{24}$$

where

$$[T_{y1u1}] = \begin{bmatrix} W_1 S \\ W_3 T \end{bmatrix} \tag{25a}$$

$$[S] = [I + \hat{G}K]^{-1} \tag{25b}$$

$$[T] = [\hat{G}K][I + \hat{G}K]^{-1} \tag{25c}$$

The infimum is chosen over all stabilizing controllers $[K]$. $[W_1]$ and $[W_3]$ are the weighting matrices for the performance and robustness. $[S]$ is the sensitivity matrix, $[T]$ is the complementary sensitivity matrix (or closed loop transfer function matrix). The singular values of $[S]$ determine the disturbance attenuation as well as the tracking performance about the reference input. The singular values of $[T]$ denote the robustness of the closed loop system about the modeling error. Since $[S]$ and $[T]$ should satisfy the following equation ;

$$[S(s)] + [T(s)] = [I] \tag{26}$$

the weighting matrices $[W_1]$, $[W_3]$ are to be chosen to satisfy the following ;

$$\bar{\sigma}([W_1(jw)]^{-1}) + \bar{\sigma}([W_3(jw)]^{-1}) > 1$$
$$\forall w > 0 \tag{27}$$

In this paper, $[W_1]^{-1}$ and $[W_3]^{-1}$ are selected to take account of not only the disturbance attenuation performance at low frequency region but also the robust stability at high frequency region ;

$$[W_1(s)]_{ii}^{-1} = \frac{k_1}{\gamma} \frac{(1+\tau_d s)}{(1+\tau_n s)}$$
$$[W_3(s)]_{ii}^{-1} = \frac{k_3}{s}, \quad i = 1, 2, 3, 4 \tag{28}$$

where γ, k_1, k_3, τ_d, τ_n are the constants which are given arbitrarily. The augmented plant $[P]$ (see Fig. 2) which consists of the system $[\hat{G}]$ and the weighting functions appropriate similar transformation ;

$$[P(s)] = \begin{bmatrix} A_0 & B_1 & B_2 \\ C_1 & D_{11} & D_{12} \\ C_2 & D_{21} & D_{22} \end{bmatrix} \tag{29}$$

where

$$[D_{11}] = [D_{22}] = [0],\ [D_{12}^T] = [D_{21}] = [0\ I]$$
$$[D_{12}^T C_1] = [0]$$
$$[B_1 D_{12}^T] = [0] \tag{30}$$

The 2-Riccati method (Safonov et. al., 1989) is used to find a stabilizing feedback control law ;

$$\{u_2(s)\} = [K(s)]\{y_2(s)\} \tag{31}$$

The controller transfer function $[K(s)]$ is written ;

$$[K(s)] = \begin{bmatrix} A_c & B_c \\ C_c & D_c \end{bmatrix} \tag{32}$$

where

$$[A_c] = [A_0] + ([B_1][B_1]^T - [B_2][B_2]^T)[P] + ([I] - [Q][P])^{-1}[Q][C_2]^T[C_2]$$
$$[B_c] = ([I] - [Q][P])^{-1}[Q][C_2]^T$$
$$[C_c] = -[B_2]^T[P]$$
$$[D_c] = [0]$$
$$[P][A_0] + [A_0]^T[P] - [P]([B_2][B_2]^T - [B_1][B_1]^T)[P] - [C_1]^T[C_1] = [0]$$
$$[Q][A_0]^T + [A_0][Q] - [Q]([C_2]^T[C_2] - [C_1]^T[C_1])[Q] - [B_1][B_1]^T = [0]$$
$$\lambda_{\max}([Q][P]) < 1$$

$[P]$, $[Q]$ are the positive semidefinite matrices. The MATLAB Toolbox is used to solve this problem.

The electric currents required for aeroelastic control are calculated in this paper. When the voltage $\{u\}$ applied to the actuators harmonically with the frequency w and the measured current $\{I\}$ are

$$\{u\}=\{V_0\}sin(wt),\ \{I\}=\{I_0\}sin(wt+\phi) \tag{33a, b}$$

the admittance matrix $[Y]$ of the model can be written as

$$\begin{aligned}[Y(jw)]&=jw\Big[[\tilde{C}_f][jwI-\tilde{A}_f]^{-1}[\tilde{B}_f]\\&\quad+[\tilde{D}_f]\Big]/k_s\\&=jw[\hat{G}_f(jw)]/k_s\end{aligned} \tag{34}$$

$\{V_0\}$ and $\{I_0\}$ are the amplitude of the voltage and current respectively. For the calculation of the electric current, it is assumed that the forces $\{u_r\}$ are exerted harmonically with the magnitude of $\{V_r\}$ on the surface of self-sensing actuator;

$$\{u_r\}=\{V_r\}sin(wt) \tag{35}$$

The required electric current can be obtained as;

$$\begin{aligned}&\{I_0\}\\&=[I+\hat{G}_f(jw)K(jw)]^{-1}[Y(jw)]\{V_r\}\end{aligned} \tag{36}$$

4. Numerical Examples

A simple wing model is used to design the control system for flutter suppression. The wing is idealized as a laminated plate model with four sets of the segmented piezoelectric materials as shown in Fig. 1. The span and chord of the model are 12 and 6 inches respectively. The laminate has six symmetric layers, $[105/\pm45]_s$ and each layer has uniform thickness, which is 0.02 *inch*. It is assumed that a set of actuators is bonded on both top and bottom surfaces of the laminated plate to generate a pure bending force for control. Each piezo sensor/actuator is sized 1.5×3.0 *inches*. Thickness of the piezoelectric materials is 0.005 *inch*, which is about 4.2% of the plate thickness. The material properties of the composite materials and piezoelectric materials are given in Table 1. A model with the actuator locations which have been obtained through the optimization technique subject to minimize the control performance index is considered as the model (Nam et. al., 1995). The x and y coordinates of the model are $pzx(i)=0.000,\ 0.003,\ 4.496,\ 2.354$ *inches* and $pzy(i)=0.000,\ 9.000,\ 0.000,\ 8.192$ *inches*. For calculation of the pressure distribution on the oscillating plate wing model undergoing simple harmonic motion, the model is divided into total 50 panels arranged 10 in the spanwise direction and 5 in the chordwise direction. The open loop flutter analysis is conducted and flutter occurred at about $615 fps\ (feet/sec)$ by the torsional mode, $w_f=57 Hz$ (Nam et. al., 1995). The design air speed required for the control system design is set to be $V_{DESIGN}=800$ *fps*.

Table 1 Material properties

Composite materials	Piezoelectric materials
$E_1=14.21\times10^6 psi$	$E_p=9.137\times10^6 psi$
$E_2=1.146\times10^6 psi$	$\rho_p=0.28 lb/in^3$
$G_{12}=0.8122\times10^6 psi$	$\upsilon_p=0.3$
$\bar{\rho}=0.05491 lb/\text{in}^3$	$d_{31}=d_{32}=6.5\times10^{-9} in/V$
$\upsilon_{12}=0.28$	$\varepsilon_{33}=3.81\times10^{-10} F/in$

Figure 3 shows the maximum and minimum singular values of the different models, which are the full model (18 states), reduced model with one aerodynamic state (13 states), and reduced model without aerodynamic states (12 states), respectively. As shown in figure, the differences between the full model (18 states) and the reduced model (13 states) are negligible over the entire frequency range. Howeveer, when the aerodynamic states are neglected for the model reduction (12 states), the error becomes significant. The reduced model with 12 states is not adequate for the control system design.

The parameters in weighting matrices $[W_1]$ and $[W_3]$ are chosen to meet the given design specifi-

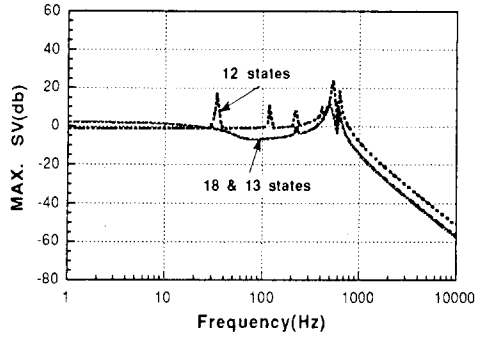

(a)

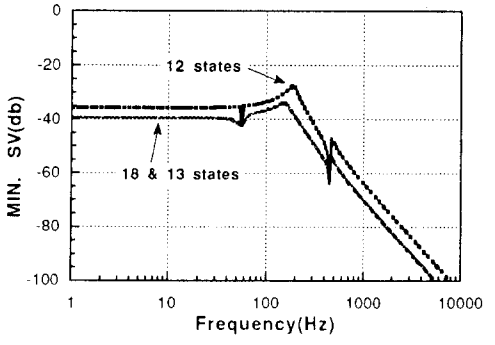

(b)

Fig. 3 Singular value plots of the full model and the reduced order model, (a) Maximum singular values. (b) Minimum singular values.

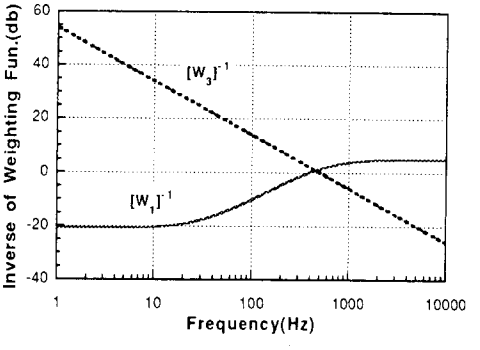

Fig. 4 Singular value specifications of weighting functions.

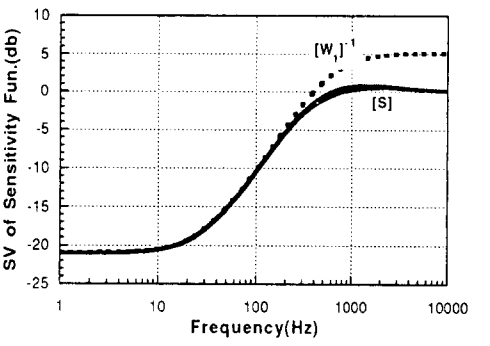

(a)

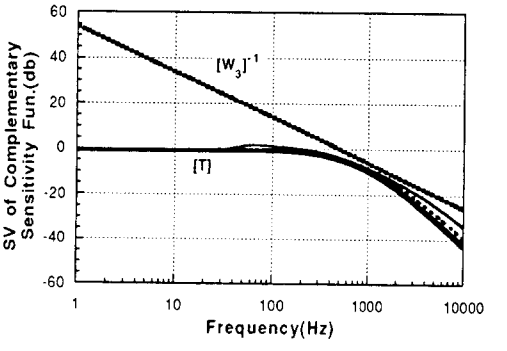

(b)

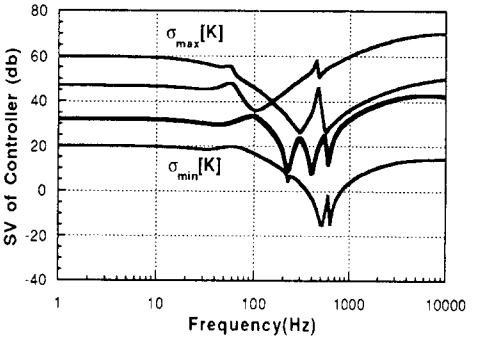

(c)

Fig. 5 Performance of the closed loop systems, (a) Sensitivity function [S] and weighting function $[W_1]^{-1}$. (b) Complementary sensitivity function [T] and weighting function $[W_3]^{-1}$. (c) Controller [K].

cation. These are $k_1=0.1$, $\tau_d=5.305\times10^{-3}$, $\tau_n=2.653\times10^{-4}$, $k_3=3.142\times10^3$. γ is the parameter on which we iterate for design. The frequency response of $[W_1]^{-1}$ and $[W_3]^{-1}$ are shown in Fig. 4. The imposed design specifications are ;

1. The error due to disturbance should be attenuated at least 1/10 in the specified frequency range from 0 to $30Hz$ after feedback loop is closed.
2. The control loop bandwidth should be 500

Hz with $-20db/decade$ roll-off above the specified frequency range.

The singular values of the sensitivity function $[S]$, the complementary sensitivity function $[T]$ and the H_∞ controller $[K]$ for the closed loop system are shown in Fig. 5. For this plot, γ is set to be 1.1 and $\| [T_{y1u1}] \|_\infty$ is 0.998, which is coincident with optimal value 1.0. Those are nearly coincident with their associated weighting functions $[W_1]^{-1}$ and $[W_3]^{-1}$, respectively. That means that the specified value of γ is close to the optimal value.

Figure 6(a) shows the step response when the unit step reference input is exerted on the actuator 1 (placed at inboard & leading edge direction of the model). The outputs track the reference inputs without excessive overshoot. In order to see the

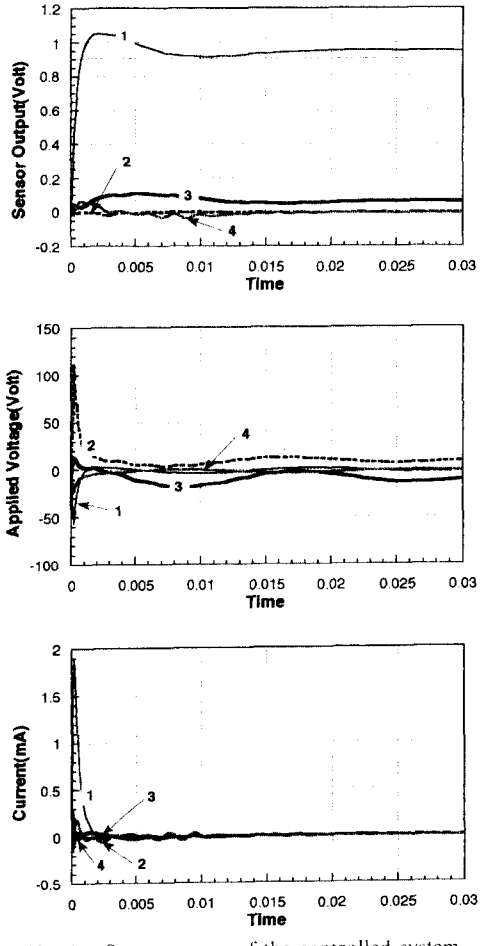

Fig. 6 Step response of the controlled system.

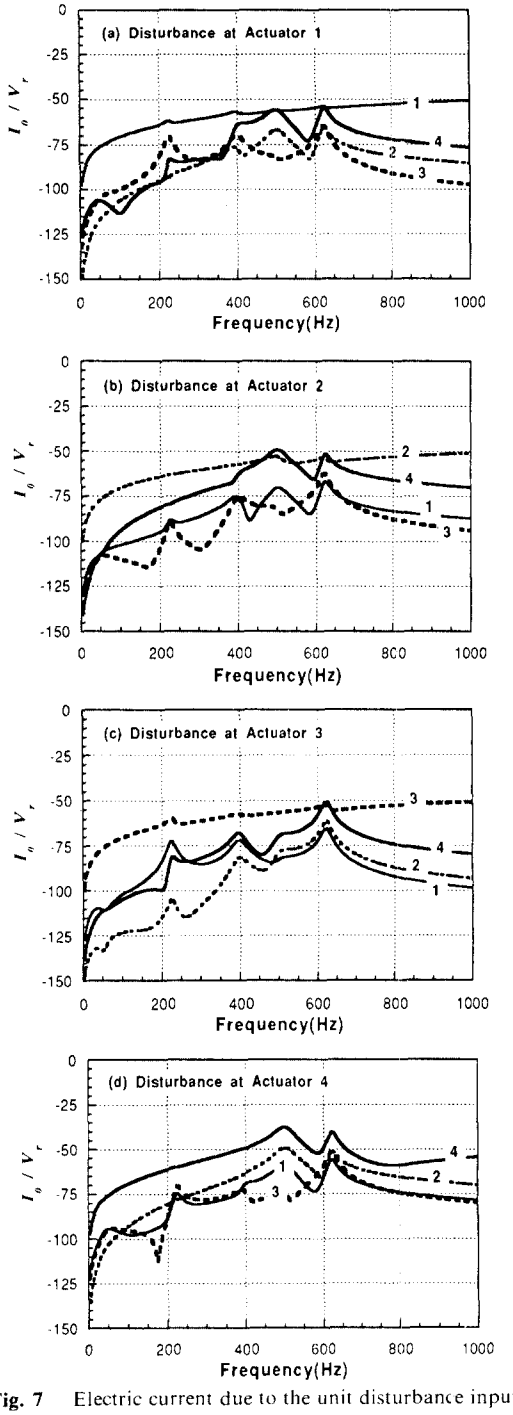

Fig. 7 Electric current due to the unit disturbance input voltage. (unit:db)

required power for control, the electric voltages and currents are calculated and the results are also shown in Fig. 6(b), (c).

When the force of the unit magnitude $\{V_r\}_j$ which is equivalent to 1 Volt actuation is exerted harmonically on the j-th actuator, the required electric currents are equal to the frequency response functions which represent the relations between the disturbance forces and the electric currents. The magnitude of the frequency response function matrix (Eq. (36)) is plotted in Fig. 7. Note that Fig. 7 represents the apparent value of $\{I_0\}_i/\{V_r\}_j$. Therefore, the real dissipative currents are less than the presented values. The diagonal elements are somewhat larger than the off-diagonal temrs due to the dielectric terms. The currents become larger at near natural frequency. But the magnitudes are less than -60 db in the frequency range from 0 to $400Hz$. Therefore, the required power per actuator will be less than 10 Watts, if the disturbance forces are 100 Volts in magnitude.

Figure 8(a), (b) show the root loci for the open loop and the closed loop when the control system is designed by using H_∞ theory with design velocity $V_{DESIGN}=800fps$. The root loci of the closed loop system indicates that the system is stable up to the speed of $1000fps$. The increase in the flutter speed compared with the open loop system is remarkable. The figures also show that the control system is robust on the unmodeled dynamics although only one aerodynamic state is included in the reduced order control model.

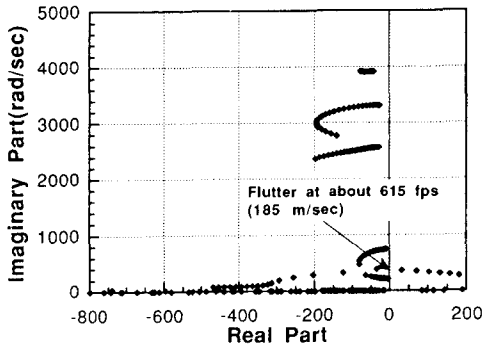

(a)

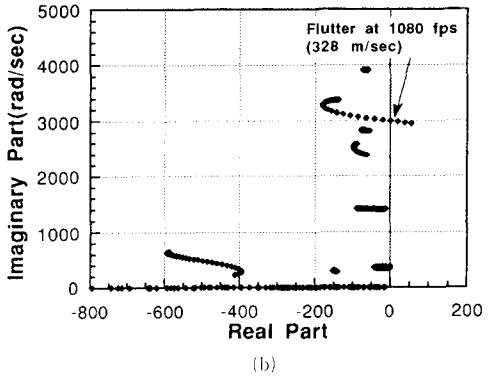

(b)

Fig. 8 (a) The open loop root loci. (b) The closed loop root loci.

5. Summary

In this paper, a control system is designed for flutter suppression of a composite wing using segmented piezoelectric self-sensing actuators. The control system uses the integrated and collocated piezoelectric self-sensing actuator pairs so as to prohibit the non-minimum phase model and the spillover due to the unmodeled dynamics. The reduced order model is developed in order to design active flutter suppression system. One of the aerodynamic states, which is a dominant state, is considered as the equivalent aerodynamic one and other aerodynamic ones are considered as modeling error. In this paper, the model reduction is performed with the stable modes by using the internal balancing method. Based on the mixed-sensitivity H_∞ control method, the control parameters are determined. For a given simple wing model, the performance of the controlled system is shown in the frequency as well as time domain. The electric current and the electric power which are required for aeroelastic control are predicted. Further study might be needed concerning the power requirement for aeroelastic control using the realistic wing structures.

References

Albano, E. and Rodden, W. P., 1969, "A Doublet-Lattice Method for Calculating Lift Distributions on Oscillating Surfaces in Subsonic flows." *AIAA Journal,* Vol. 7, No. 2, Feb. pp. 279 ~285.

Doyle, J. C., Glover, K., Khargonekar, P. P and Francis, B. A., 1989, "State-Space Solutions to Standard H_2 and H_∞ Control Problems," *IEEE Transactions on Automatic Control,* Vol. 34, No. 8, pp. 831~847.

Ehlers, S. M. and Weisshaar, T. A., 1992, "Effects of Adaptive Material Properties on Static Aeroelastic Control," AIAA Paper No. 92-2526, *Proceedings of the 33th Structures, Structural Dynamics and Material Conference,* TX, April. pp. 914~924

Glover, K. and McFarlane, D., 1989, "Robust Stabilization of Normalized Coprime Factor Plant Descriptions with H_∞-Bounded Uncertainty," *IEEE Transactions on Automatic Control,* Vol. 34, No. 8. pp. 821~830

Hoadley, S. T. and Karpel, M., 1991, "Application of Aeroservoelastic Modeling Using Minimum-State Unsteady Aerodynamic Approximations," *Journal of Guidance, Control, and Dynamics,* Vol. 14, No. 6, pp. 1267~1276.

Leeks, T. J. and Weisshaar, T. A., 1994, "Optimizing Induced Strain Actuators for Maximum Panel Deflection," AIAA Paper No. 94 -1774, *Proceedings of the AIAA/ASME Adaptive Structures Forum,* SC, April. pp.378 ~387.

Leeks, T. J. and Weisshaar, T. A., 1995, "Optimization of Unsymmetric Actuators for Maximum Panel Deflection Control," *Proceedings on Smart Structures and Materials '95,* SPIE, San Diego, CA, March. pp. 62~75

Lin, C.Y. and Crawley, E. F., 1994, "Towards Optimal Aeroelastic Control Using Elastic and Induced Strain Anisotropy," AIAA Paper No. 94 -1547, *Proceedings of the 35th Structures, Structural Dynamics and Material Conference,* SC, April. pp. 1781~1792.

Moore, B. C., 1981, "Principal Component Analysis in Linear Systems : Controlability, Observability, and Model Reduction," *IEEE Transactions on Automatic Control,* AC-26, pp. 17 ~31.

Nam, C., Kim, Y. and Weisshaar, T. A., 1995, "Optimal Sizing and Placement of Piezo Actuators for Active Flutter Suppression," *Proceedings on Smart Structures and Materials '95,* SPIE, San Diego, CA, March. pp. 40~51.

Nam, C. and Kim, Y., 1995, "Optimal Design of Adaptive Composite Lifting Surface for Flutter Suppression," *AIAA Journal,* Vol. 33, No. 10, Oct. pp. 1897~1904.

Safonov, M. G., Limebeer, D. J. N. and Chiang, R. Y., 1989, "Simplifing the H_∞ Theory via Loop Shifting, Matrix Pencil and Descriptor Concepts," *International Journal of Control,* Vol. 50, No. 6, pp. 2467~2488.

Suleman, A. and Venkayya, V. B., 1994, "Flutter Control of Adaptive Composite Panel," AIAA Paper No. 94-1744, *Proceedings of the AIAA/ASME Adaptive Structures Forum,* SC, April. pp. 118~126.

Zhou, S., Liang, C. and Rogers, C. A., 1994, "Coupled Electro-Mechanical Impedence Modeling to Predict Power requirement and Energy Efficiency of Piezoelectric Actuators Integrated with Plate-Like Structures," AIAA Paper No. 94 -1762, *Proceedings of the AIAA/ASME Adaptive Structures Forum,* SC, April. pp. 259 ~269.